

D. Priya, S. Thirumaran

## Investigation and Study of CaO-Borate Glass

Manomaniam Sundaranar University, Tirunelveli, India, [geetha.palani@dce.edu.in](mailto:geetha.palani@dce.edu.in)  
Department of Physics, Annamalai University, Chidambaram, India, [vaishuu.geethu@gmail.com](mailto:vaishuu.geethu@gmail.com)

Recent days the special interest towards Glasses is specifically due to their vast applications that they range. Glass series Calcium borate metallic glass ( $\text{CaO-B}_2\text{O}_3$ ) has been prepared by melt quenching technique. CaO influences like density/molar volume ratio on the properties have analyzed and glass sample different modulus has found between them. The optical properties such as direct and indirect bandgap, Urbach energy, band gap, which also includes heat-treated glasses, has studied by Fourier transform infrared spectroscopy and UV-visible, respectively. According to this model elastic moduli increase, this is because of the CaO content increase. The Debye temperature, elastic moduli, other acoustic parameters and Poisson's ratio has acquired from experimental data. The obtained results show that the CaO enters into the glass network as a modifier by occupying increasing the nonbridging oxygen atoms (NBOs) and the interstitial spaces in the network.

**Keywords:** metallic glasses; acoustical parameters; Debye temperature; elastic moduli; optical properties.

Received 11 May 2021; Accepted 17 June 2021.

### Introduction

A heavy metal based glass has attracted noticeable interests because of their potential applications.  $\text{B}_2\text{O}_3$  containing glass exhibits high optical basicity, possesses higher refractive index, large nonlinear optical susceptibility and large polarizability [1].  $\text{B}_2\text{O}_3$  in borate glasses is a perfect glass former due to its lower cation size, higher bond strength, valence of  $\text{B}_2\text{O}_3$  and smaller heat of fusion to be considered as the highest tendency of glass formation due to molten  $\text{B}_2\text{O}_3$  does not crystalline by itself even when cooled at a slowest rate. The  $\text{B}^{3+}$  ion size is very small easily fit into the void of trigonal created by three oxide ions in mutual contact, to form  $\text{BO}_3$  units. And there is a primary building block in all borate glasses. These glasses find wide applications in optoelectronic devices layer, glass ceramics field, reflecting windows, mechanical and thermal sensors etc. For the past many years Differential thermal analysis and Infrared spectroscopy is also utilized as important tools to study the glasses nature [2-3]. Fourier transform infrared spectroscopy have become important tool for resolving the local arrangement structure in glasses [4] and it is utilized from a very long period to find the different glasses

structure. Borate glasses physical properties with structural properties can often be changed by the network modifier addition to the basic constituents. The ultrasonic parameters measurement like velocities, acoustical impedance, microhardness and Poisson's ratio as a function of composition is showing unnoticeable interest for the characterization of whole glasses also they provide noticeable information about structural changes, coordination, and cross link density [5-6]. The acoustical properties are incompletely reasonable for representing composition function of glasses because they are providing some data of micro structure and glasses dynamics. To find microstructure examination, mechanical properties characterization, and the phase changes ultrasonic Non Destructive Testing (NDT) has found to be the best methods and to assess elastic constants [7-8]. In this paper, BSC glass system is discussed, ( $\text{B}_2\text{O}_3 - \text{Na}_2\text{CO}_3 - \text{CaO}$ ).

The ultrasonic velocity and density for the glass systems have been measured by pulse echo technique by Archimedes' principle. The elastic constants like Shear modulus (S), longitudinal modulus (L), Poisson's ration ( $\sigma$ ), bulk modulus (K), Young's modulus (E), acoustic impedances (Z), micro hardness (H), Debye temperature

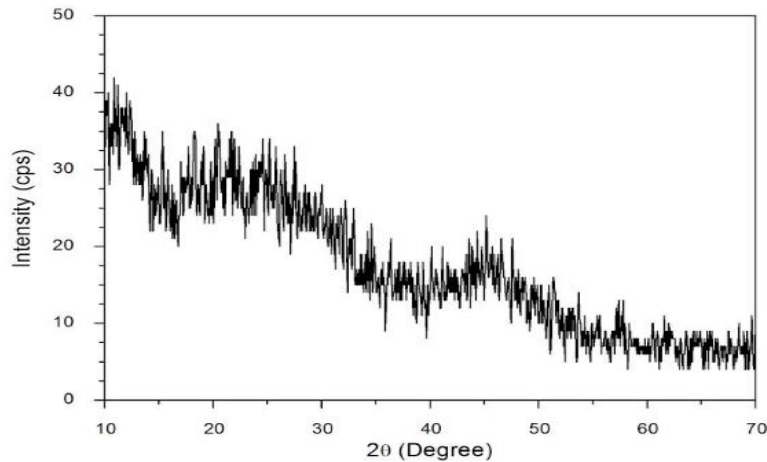


**Fig. 1.** XRD pattern of BSC glass system.

( $\theta_D$ ), and co-efficient of thermal expansion ( $\alpha_p$ ) has measured which gives more important information about the rigidity and borate glass structure. The XRD, spectroscopic, scanning electron microscopic (SEM) and UV studies to substantiate their structural elucidation analysis are also been carried out for the glass and presented in this paper.

## I. Experimental Details

The current research work chemicals (AR, SR grade) were used with 99 % least measure was gotten. The appropriate mixture homogenization of the chemicals component was affected by consistently granulated. The blend is heated with the help of platinum crucible and temperature is controlled through a muffle furnace after few hours at certain point it was raised step by step to at the rate of 100k/hour in higher temperature, BSC glass system glassily structure is formed at 1400 K. With the help of heavy copper molding block having the 5 mm dimension diameter and length of 10 mm, molten glass melt was quickly poured and kept at room temperature without any disturbance. To avoid the mechanical strains formed during the quenching process the glass sample was annealed for two hours at 400 K. The glass two opposite faces were polished highly to ensure a good parallelism. To remove the presence of any foreign particles all glasses were cleaned with acetone. The samples are prepared by non-hygroscopic and chemically stable, those glass samples system (BSC) are taken for analysis in plate.

## II. Results

### 2.1. XRD Studies

X-Ray Diffraction (XRD) analysis was done for the glass sample prepared to confirm the glass sample amorphous nature. PW1700: (Philips Eindhoven, the New Netherlands) X-ray diffractometer was utilized with CuK as a radiation source between  $20^\circ$  and  $80^\circ$  to get the results. The glass sample was washed and then the washed samples were dried, ground, at room temperature and later utilized to get the x-ray diffraction patterns. From the

spectrum obtained we can clearly see the unmelted crystalline particles which confirm the amorphous nature, and also BSC glass system structure is plotted in Figure 1.

### 2.2. Spectral Analysis

IR absorption spectra of the studied samples show IR bands which are the characteristics of triangular and tetrahedral borate units together with few small bands due to water OH and B-OH. The FTIR studies show that the glass structure consists of  $\text{BO}_3$  and  $\text{BO}_4$  units. The addition of CaO modified the boroxol ring [8]. The IR absorption spectra of the present glasses were recorded in the range  $400 - 4000 \text{ cm}^{-1}$  shows the normalized FTIR absorption of calcium borate glasses. The observed infrared spectra of the glasses arise largely from the modified borate networks and are mainly active in spectral range  $400 - 600 \text{ cm}^{-1}$ . Therefore the spectra are shown in  $450 - 2000 \text{ cm}^{-1}$  range for better clarity. The boron ion is a glass network forming action and it may occupy the centers of oxygen triangle or tetrahedral.

The IR analysis of the borate glasses in general shows four distinct regions shown in Fig. two regions from  $1200 - 1600 \text{ cm}^{-1}$  and from  $800 - 1200 \text{ cm}^{-1}$  are assigned to the stretching vibrations of both triangular  $\text{BO}_3$  and tetrahedral  $\text{BO}_4$  borate units respectively. Deformation modes of both types of units are active between  $600 - 800 \text{ cm}^{-1}$ . Accordingly the systematical changes in the infrared spectra of the glasses under study showed the presence of three principle broad bands at around  $700, 1000$  and  $1400 \text{ cm}^{-1}$  as shown in figure [4]. The peak around  $700$  is assigned to bending vibrations of B-O linkages in the borate network. The band between  $825$  and  $1130 \text{ cm}^{-1}$  are assigned to the B-O stretching vibrations of tetrahedral  $\text{BO}_4$ . The band at around  $1260 \text{ cm}^{-1}$  is assigned to the stretching vibrations of the B-O bonds of  $\text{BO}_3$  involving mainly the linkage oxygen connecting different groups. The bands observed at  $1350 - 1450 \text{ cm}^{-1}$  are due to the stretching vibrations of the B-O of  $\text{BO}_3$  units in metaborate, pyroborate and orthoborates [9-10].

The peaks are appeared at around  $1560 - 1580 \text{ cm}^{-1}$  is assigned as antisymmetrical stretching vibrations of  $\text{BO}_3$  units. The peak observed at  $1650 \text{ cm}^{-1}$  indicates that  $\text{BO}_3$  changes to  $\text{BO}_4$  and also the peak may be assigned to bending vibrational mode of molecular water. Most of the

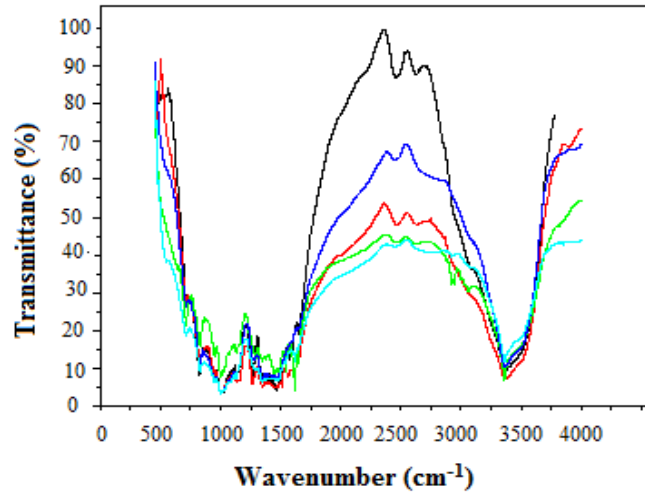


Fig. 2. Vibrational analysis of BSC glass system.

Table 1

Vibrational analysis band position comparison and their assignments

Band position					Assignments
S2C1	S2C2	S2C3	S2C4	S2C5	
3412	3417	3435	3429	3422,3013,2952	Antisymmetric&symmetric stretching vibration of H <sub>2</sub> O molecules
2744	2754	2693	2693	2851	
1625	1611	1578,1419		1624	Bending vibration of H <sub>2</sub> O molecule, B-O stretching vibrations from BO <sub>3</sub> to BO <sub>4</sub> triangles of BO <sub>4</sub> units.
				1579,1456	B-O stretching vibrations from BO <sub>3</sub> units, varied types of borate.
1391	1364		1374	1383	B-O stretching vibrations of trigonal units
1050		1267,1028	1057	1039,1022	BO <sub>4</sub> B-O stretching vibrations from tri,tetra, &pentaborate
907					B-O stretching vibrations of BO <sub>4</sub> units
		712		709,649,613	B-O-B bending vibrations in BO <sub>4</sub> units.
689			689		CaO Stretching vibrations
606				601	Deformation modes of Borate

inorganic materials occur in hygroscopic form so; the peaks established around at 3360 - 2636 cm<sup>-1</sup> are assigned as antisymmetric and symmetric stretching vibration of H<sub>2</sub>O molecules trapped in the glasses during the experiment. In this glass samples, the peaks appeared at 659,689 cm<sup>-1</sup> is assigned as Ca-O stretching vibrations [11]. The vibrational assignments of borate glasses are shown in table. The FTIR study shows that the glass network consists of BO<sub>3</sub>& BO<sub>4</sub> units. CaO act as modifiers. Generally Ca<sup>2+</sup> ions occupy the interstitial positions. Table 1 shows the vibrational analysis band position comparison and their assignments.

Most of the inorganic materials occur in hygroscopic form so; the peaks established at 3360 - 2636 cm<sup>-1</sup> are shows symmetric stretching vibration and antisymmetric of water molecules found in the glasses [12].

### 2.3. UV-Vis Analysis

The borate glasses absorption spectra in the wavelength region 0 - 2200 has been recorded. The

intense and the broad absorption band from 230 - 2200 nm are related to the Ca ions in distorted sites of the borate glass network. The optical band energy was found to be dependent upon the variation of CaO content [13]. The wavelength maximum and the band gap energy of various concentrations of glass samples are shown in Table 2.

Table 2

Wavelength maximum and the band gap energy of various concentrations of glass samples

System	Wavelength minimum(nm)	Bandgap (eV)
S2C1	214	5.77
S2C2	255	4.84
S2C3	239	5.16
S2C4	231	5.34
S2C5	239	5.16

Small change in band maxima due to small structural change in the glass matrix with increase in CO<sub>3</sub> content is

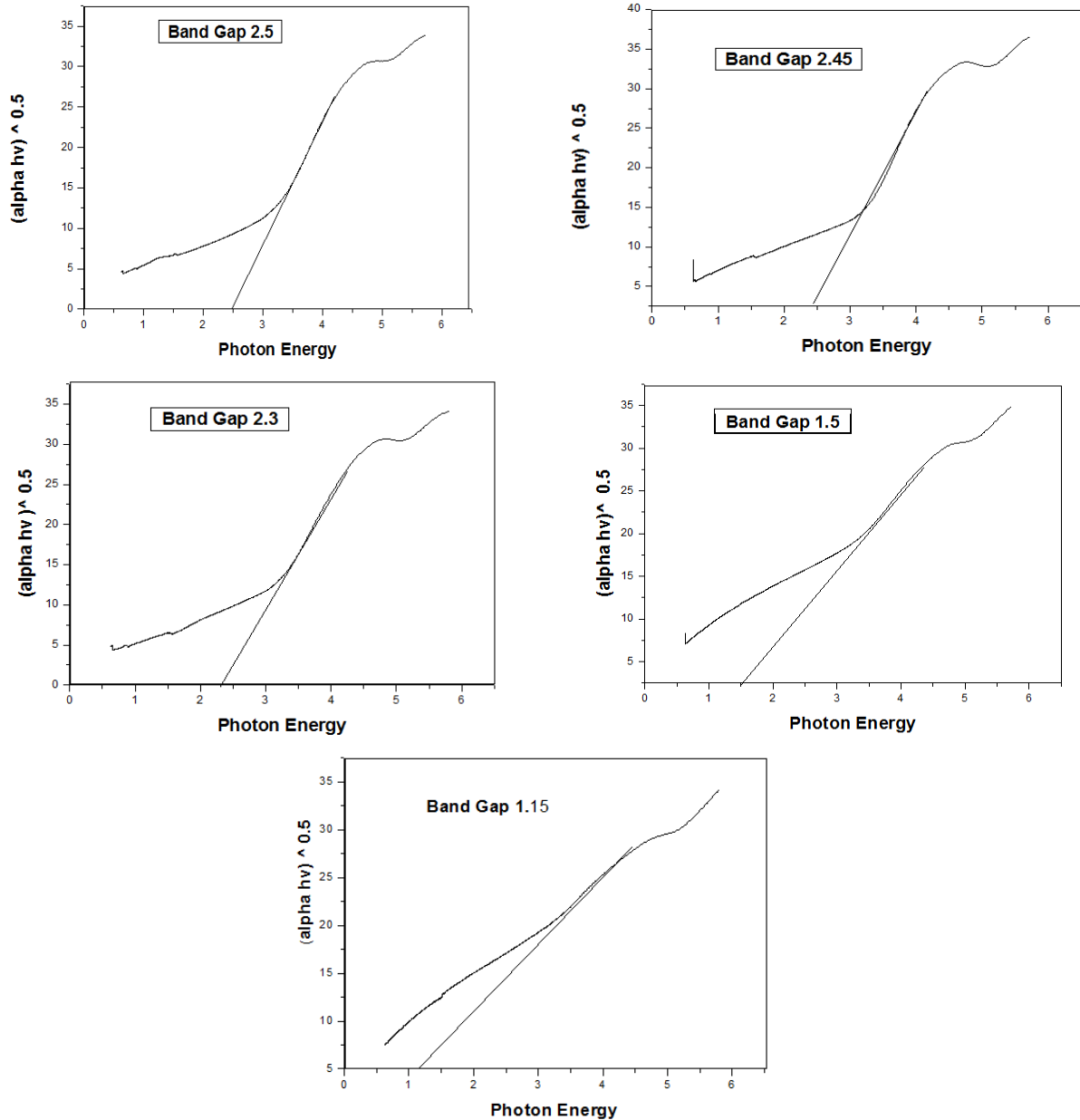


Fig. 3. Direct band gap and indirect band gap graph for the prepared sample.

observed.

For photon energies  $h\nu$  just above the fundamental edge, the absorption  $\alpha$  follows the standards relation,  $\alpha = (h\nu - E_g)^{1/2}/A$ , where  $A$  is a constant and  $E_g$  is defined as the energy band gap. The value of  $E_g$  indirect transitions is obtained by extrapolation of  $(\alpha h\nu)^{1/2}$  versus  $h\nu$  plot to  $\alpha^{1/2} = 0$ . (2h3). Figure 3 shows the plots for direct band gap and indirect band gap for the prepared sample and their values and the values are tabulated in table [3]. In BSC glass system photon energy decreases with increasing CaO content. The addition of sodium ions increase localized electrons because of an increase in donor center in glass network, the presence of higher concentration of these donor centers decreases the optical band gap. In this glass system BSC CaO are glass modifiers [14]. The addition of alkaline earth oxides and many other divalent metal oxides causes depolarization of the glass chain.

Table 3

Direct band gap and indirect band gap for the prepared samples

Mol %	Direct Bandgap	Indirect Bandgap
	CaO	CaO
08	3.64	2.50
11	3.40	2.45
14	3.45	2.30
17	3.42	1.50
20	2.95	1.15

#### 2.4. Density

In the field of science especially where the glass structure is concerned density plays an important physical property. The measurement of density is a sensitive tool which can easily find any structural change in the glass network. The CaO are modifiers network and present in  $B_2O_3$ - CaO glass interstitially and breakdown bridging

Table 4

Different glass specimens ultrasonic velocity [both longitudinal and shear] and density values with respect to mol% CaO change

Name of the sample	Density $\rho/(\times 10^3 \text{ kg. m}^{-3})$	Ultrasonic Velocity $U/(\text{m.s}^{-1})$		Elastic moduli			
		Longitudinal ( $U_l$ )	Shear ( $U_s$ )	Longitudinal $L/(\times 10^9 \text{ N.m}^{-2})$	Shear $G/(\times 10^9 \text{ N.m}^{-2})$	Bulk $K/(\times 10^9 \text{ N.m}^{-2})$	Young's $E/(\times 10^9 \text{ N.m}^{-2})$
S2C1	2413.4	3949.35	2169.77	37.6	11.4	22.5	29.2
S2C2	2387.9	3929.9	2159.08	36.9	11.1	22.0	28.6
S2C3	2345.9	3888.56	2136.37	35.5	10.7	21.2	27.5
S2C4	2275.1	3782.79	2078.26	32.6	9.83	19.5	25.2
S2C5	2257	3694.46	1980.33	30.8	8.85	19.0	23.0

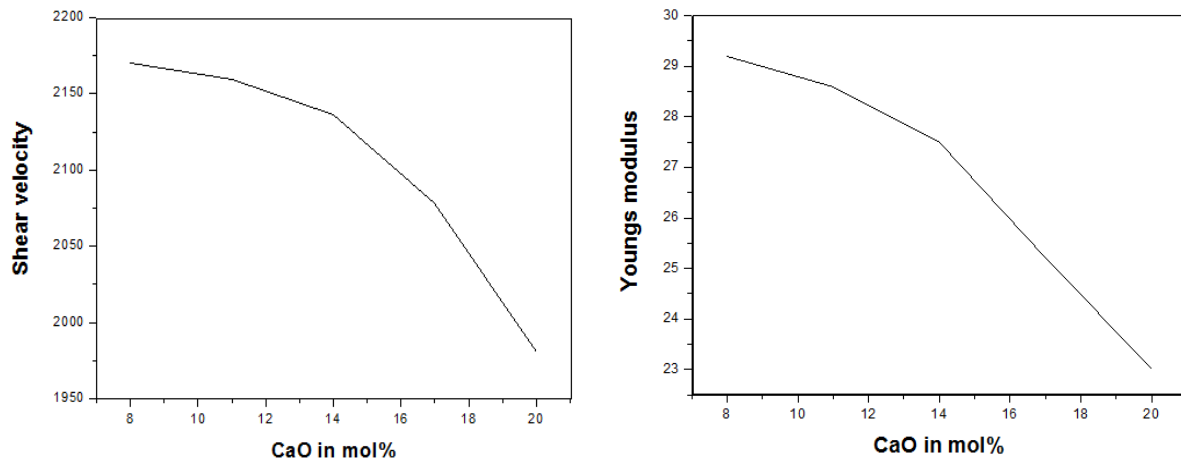


Fig. 4. Elastic behavior of BSC glass system.

bonds. The non-bridging oxygen's creation in the network is reduced decrease and connectivity density. Decreasing density values in the glass system of BSC may also be interpreted because of the  $\text{BO}_4$  unit formation due to inclusion of metal ion CaO contents. However, the inclusion of sodium ions CaO which positioned in the cavities of an empty band gap space of the network obstructing the formation of  $\text{BO}_4$  unit further and this makes the density to decrease [15]. The decreases in density assure the less compact structure of the glass.

### 2.5. Ultrasonic behavior of BSC glass systems

It is observed that both shear and longitudinal velocities of BSC systems mol % is lowering with increase of CaO respectively. The ultrasonic velocity decrease is connected with the number of non-bridging oxygen (NBO) increase and at the same time glass network connectivity decrease. It may also be interpreted as the decreasing velocities in BSC glass systems and it can be interpreted as due to the involvement of CaO ions as modifiers breaking up  $\text{B}_2\text{O}_3$  units and  $\text{O}_2$  of CaO ions tetrahedral bonds [16]. Consequently, resulting in replacing of its symmetry of  $\text{B}_2\text{O}_3$  and its cations occupy the interstitial position. Rupturing the symmetry of tetrahedral  $\text{B}_2\text{O}_3$  network and a creation of negative changed atoms leads to the decrease in ultrasonic velocity, the inclusion of heavy metal leading the wave for decrease of ultrasonic velocities in the glassy matrix which results

in ultrasonic wave's lower impedance to the propagation in the specimen. The different glass specimens ultrasonic velocity [both longitudinal and shear] and density values with respect to mol % CaO change and The elastic moduli such as longitudinal modulus (L), shear modulus (G), bulk modulus (K), and young's modulus (E) are tabulated in Table 4.

### 2.6. Elastic behavior of BSS glass systems

The elastic properties field information forces regarding that operate in the middle of ions or atoms in the solid materials. Kind of this information provides predominant clues in understanding and interpreting solid materials bonding nature. These properties help in explaining the glass structure as a function and its dimensionality, composition and the connectivity of glass structure. The elastic moduli decrease has been assigned to the non-bridging oxygen's presence and the glass network connectivity decrease. The elastic behavior graph is shown in Figure 4.

### 2.7. Poisson's Ratio

In elastic analysis of materials Poisson's ratio play a significant material property. From the survey results observed where changes in cross-link density of the glass network Poisson's ratio is affected and suggested that structure having large density cross link will have in the order of 0.1 to 0.2 Poisson's ratio while structures with

Table 5

Poisson's ratio ( $\sigma$ ), acoustic impedance ( $Z$ ), microhardness ( $H$ ), Debye temperature ( $\theta_D$ ) and thermal expansion coefficient ( $\alpha_p$ ) values for the glass systems BSC

Name of the sample	Poisson's ratio ( $\sigma$ )	Acoustic impedance $Z/$ ( $\times 10^7 \text{ kg.m}^{-2} \text{ s}^{-1}$ )	Microhardness $H/$ ( $\times 10^9 \text{ N.m}^{-2}$ )	Debye temperature $\theta_D/(\text{K})$	Thermal expansion coefficient $\alpha_p/(\text{K}^{-1})$
S2C1	0.283832	0.9531	1.6434	294.23	91643.42
S2C2	0.283833	0.9384	1.6021	298.15	91249.62
S2C3	0.283833	0.9122	1.5464	309.68	90226.54
S2C4	0.283833	0.8606	1.4256	341.42	87718.35
S2C5	0.298418	0.8338	1.1934	3.62.59	85732.86

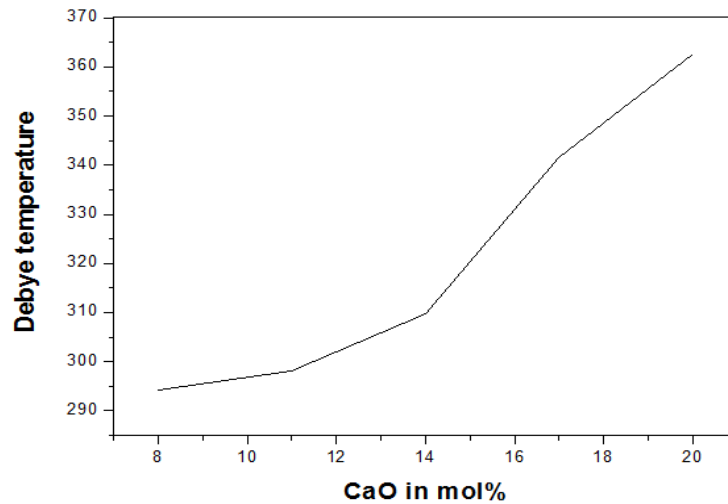


Fig. 5.A plot of CaO Vs Debye temperature.

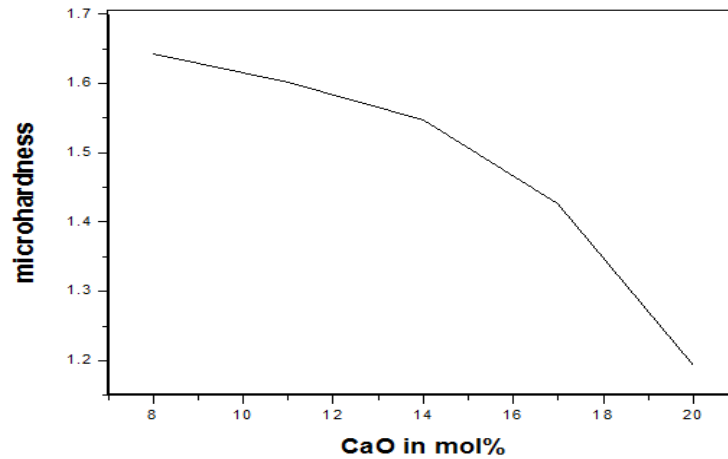


Fig. 6. Microhardness variations of glasses with CaO content.

low crosslink density in the order of 0.3 to 0.5 have Poisson's ratio. BSC glass system have Poisson's ratio 0.3 nearly and it shows that there glass structures possess low cross-link density [17]. Table 5 shows the Poisson's ratio ( $\sigma$ ), acoustic impedance ( $Z$ ), micro hardness ( $H$ ), Debye temperature ( $\theta_D$ ) and thermal expansion co-efficient ( $\alpha_p$ ) values for the glass systems BSC.

### 2.8. Debye temperature

From the measured velocity Debye temperature ( $\theta_D$ ) can be directly obtained. It increases with CaO content

mol % increase in BSC glass system and the plotted graph is shown in Figure 5. This Debye temperature rise may be because of the centre charge coming nearer than the required distance, while comparing with other data this shows a Columbian interaction more effectively. These kinds of interaction usually will result in increased energy vibrational modes, and at the same time it increases the Debye temperature [18].

### 2.9. Acoustical impedance

The acoustical impedance and the thermal expansion

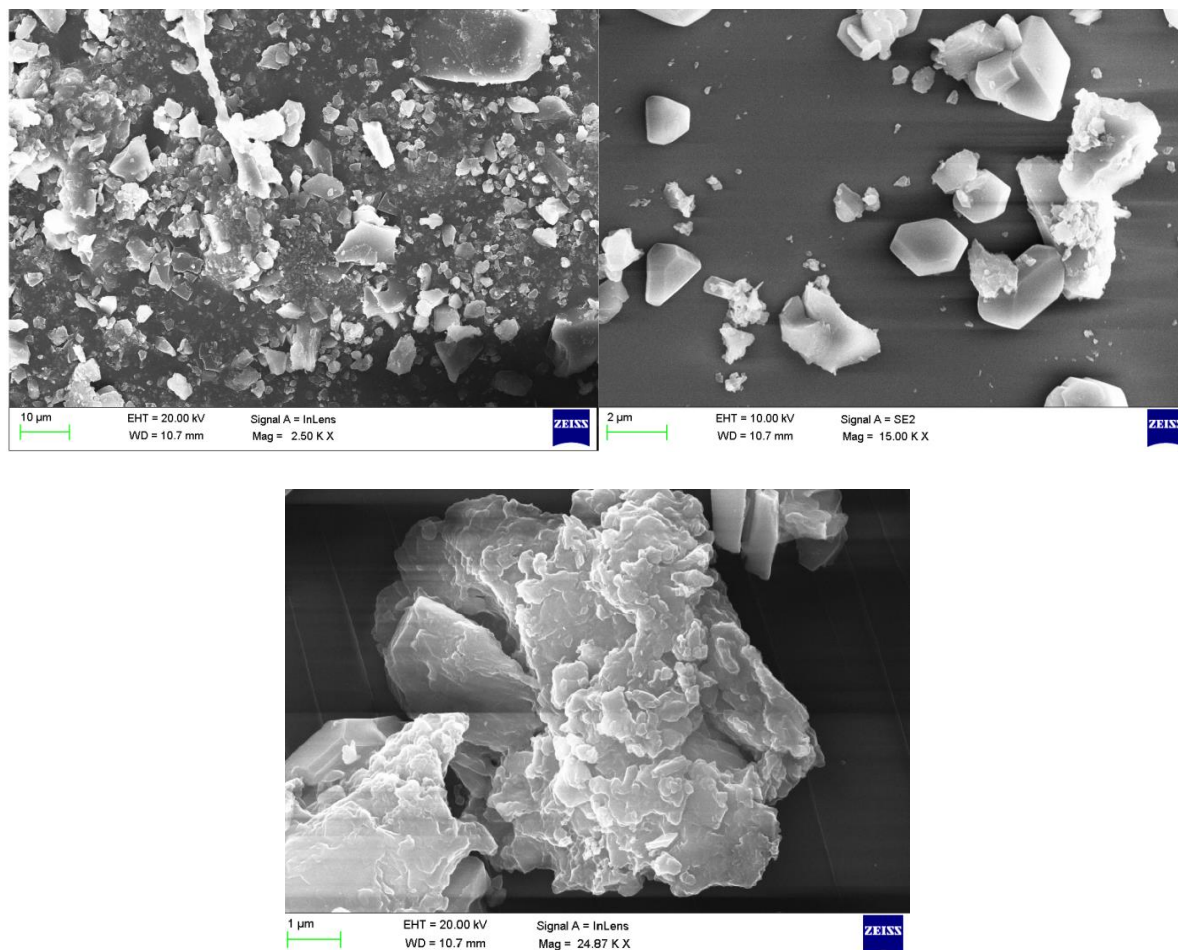


Fig. 7. SEM micrographs of BSC glass system.

coefficient decrease with CaO mol % increase in BSC glass respectively. This confirms the rigidity decrease of the glass structure. Figure 6 represents microhardness variation of glasses with CaO content. Decrease in microhardness of glasses means softening point's reduction, increases as the network modifiers content [19].

### 2.10. Scanning Electron Microscope (SEM)

To investigate the glass samples surface nature, scanning electron microscope analysis was carried out. SEM micrographs of BSC glass system are shown in the Figure 7. It is seen that various measured grain particles are disseminated. The size of the particle appears to differ in each graph obtained. By nature these particles are very spherical and angular. These photographs represent clearly that there is no existing crystalline phase in the samples overall surfaces. The huge particles might be mono mineral; however is likely to be composite majority. Some sphere like agglomerates were seen spreading on the surface of glass because of the amorphous apatite deposition. This recommends that during the formation of glass, clusters presence formed by fibers are framed [20].

Additionally, large particles may be present in the glasses, agglomerates, aggregates and bunches of clusters, which explains clearly the glass samples morphology surface.

### Conclusion

The conclusions drawn from these studies for BSC glass system are summarized as: The BSC glasses decrease with the increase in CaO content density as well as molar volume. This is due to the difference in the atomic masses of and CaO ions. X-Ray diffraction pattern shows the amorphous behavior of the prepared samples. FTIR confirmed the existence of trigonal and tetrahedral borate groups with an establishment of Bi-O bonds. The topographical aspects of the glass samples are reported from SEM micrograph. The presence of  $\text{BO}_3$  and  $\text{BO}_4$  structural units are observed from the traces of IR spectra.

*Priya D - Research Scholar, Department of Physics;*  
*Thirumarar S. - Professor, Department of Physics.*

[1] S. Ghosh, A.D. Sharma, P. Kundu, S. Mahanty, R.N. Basu, J. Non-Cryst. Solids 354, 4081 (2008); <https://doi.org/10.1016/j.jnoncrsol.2008.05.036>.

- [2] X. Yang, L. Zhang, X. Chen, X. Sun, G. Yang, X. Guo, H. Yang, C. Gao, Z. Gou, J. Non-Cryst. Solids 358,1171 (2012). <https://doi.org/10.1016/j.jnoncrysol.2012.02.005>
- [3] Manupriya, K. S. et.al., physica status solidi (a), Volume203, Issue10, August 2006, Pages 2356-2364. <https://doi.org/10.1002/pssa.200622140>
- [4] M. Tanveer, et.al, CrystEngCom **16**, 5290–5300, (2014). <https://doi.org/10.1039/C4CE00090K>
- [5] Z. Wang, C. Shu, K. Chou, Inter. J. Sci. Research. 51, 1021 (2011). <https://doi.org/10.2355/isijinternational.51.1021>
- [6] H. Doweidar, D. El-Damrawia, M. Al-Zaibania, Vibrational Spectroscopy68, 91 (2013). [10.1016/j.vibspec.2013.05.015](https://doi.org/10.1016/j.vibspec.2013.05.015)
- [7] S.S. Rojas, K. Yukimitu, A.S.S. Camargo, L.A.O. Nunes, A.C. Hernandez, J. NonCryst. Solids 352,3608 (2006). <https://doi.org/10.1016/j.jnoncrysol.2006.02.128>
- [8] A.M. Abdelghany, H.A. ElBatal, F.M. EzzElDin, Spectrochim Acta A 149,788 (2015). [10.1016/j.saa.2015.04.105](https://doi.org/10.1016/j.saa.2015.04.105)
- [9] A. Makishima, J.D. Mackenzie, J Non-Cryst Solids 17,147 (1975). [https://doi.org/10.1016/0022-3093\(73\)90053-7](https://doi.org/10.1016/0022-3093(73)90053-7)
- [10] M. Ren, S. Cai, W. Zhang, T. Liu, X. Wu, P. Xu, D. Wang, J Non-Cryst Solids 380, 78 (2013). <https://doi.org/10.1016/j.jnoncrysol.2013.09.007>
- [11] V. Rajendran, A. Nishara Begum, M.A. Azooz, and F.H. El-Batal, Biomater.4263 (2002). DOI: [10.1016/s0142-9612\(02\)00189-8](https://doi.org/10.1016/s0142-9612(02)00189-8)
- [12] B.P.C.Rao, M.T.Shyamsunder, C.Babu Rao, D.K.Bhattacharya, BaldevRaj Non-destructive Testing '92, 1992, Pages 346-350. <https://doi.org/10.1016/B978-0-444-89791-6.50075-5>
- [13] Sujata Sanshi, SaitaDuhan, Ashish Agarwal, Praveen Aghamkar, J. All. Comp. 488 454 (2009). <https://doi.org/10.1016/j.jallcom.2009.09.009>
- [14] V. Rajendran, N. Palanivelu, B.K. Chaudhuri, K. Goswami, Phys.Status Solidi A, 191,445 (2002). [10.1002/pssa.200622160](https://doi.org/10.1002/pssa.200622160)
- [15] E.A. Abou Neel, W. Chrzanowski, S.P. Valappil, J Non Cryst Solids355, 991 (2009). <https://doi.org/10.1016/j.jnoncrysol.2009.04.016>
- [16] M. Marezio, H.A. PlettingerW.H. Zachariasen, Acta Crystallographica 16(5),390 (1963). <https://doi.org/10.1107/S0365110X63001031>
- [17] C.C. Wagner, V. Ferraresi, R. CurottoPis Diez, E.J. Baran, Biological Trace Element Research 122(1), 64 (2008). <https://doi.org/10.1007/s12011-007-8060-0>
- [18] A. Makishima, J.D. Mackenzie, J. Non. Cryst. Solids 17, 147 (1975). [https://doi.org/10.1016/0022-3093\(75\)90047-2](https://doi.org/10.1016/0022-3093(75)90047-2).
- [19] V. Rajendran, F.A. Khaliifa, H.A. El-Batal, Indian J. Phys. 69A, 237 (1995). DOI: [10.1016/j.ceramint.2012.01.026](https://doi.org/10.1016/j.ceramint.2012.01.026)
- [20] D.C. Hofmann, J.Y. Suh, A. Wiest, and W. Johnson, Scripta Materialia 59(7), 684 (2008). <https://doi.org/10.1016/j.scriptamat.2008.05.046>

Д. Прайя, С. Тірумаран

## Дослідження та вивчення СаО - боратного скла

Університет Манонманіама Сундаранар, Тірунелвелі, Індія, [geetha.palani@dce.edu.in](mailto:geetha.palani@dce.edu.in)  
Університет Аннамалай, Індія, [vaishuu.geethu@gmail.com](mailto:vaishuu.geethu@gmail.com)

Останнім часом особливий інтерес до стекел викликаний їх широким застосуванням. Скло серії Кальцій-боратне металеве скло (СаО – В<sub>2</sub>О<sub>3</sub>) виготовлено методом загартування у розплаві. Проаналізовано вплив особливостей СаО, таких як співвідношення щільність / молярний об'єм, на властивості та виявлено зразки скла із різними модулями. Оптичні властивості, зокрема, пряма та непряма ширина забороненої зони, енергія Урбаха, включаючи також і термооброблені стекла, вивчали за допомогою перетворення Фур'є інфрачервоної спектроскопії та УФ-діапазону, відповідно. Згідно із запропонованою моделлю модулі пружності збільшуються. Це пов'язано зі збільшенням вмісту СаО. З експериментальних даних отримано значення температури Дебая, модулі пружності, інші акустичні параметри та коефіцієнт Пуассона. Результати показують, що СаО потрапляє в скляну матрицю, як модифікатор, займаючи позиції немежевих атомів кисню (NBO) та міжатомних порожнин.

**Ключові слова:** металеві стекла; акустичні параметри; температура Дебая; модуль пружності; оптичні властивості.